Modern Pathology (2015) 28, 1470–1480

Periductal stromal collagen topology of pancreatic ductal adenocarcinoma differs from that of normal and chronic pancreatitis

Cole R Drifka[1,2], Jo Tod[3], Agnes G Loeffler[4,5], Yuming Liu[2], Gareth J Thomas[3], Kevin W Eliceiri[1,2,5] and Kao W John[1,2,5,6,7]

[1]Department of Biomedical Engineering, University of Wisconsin, Madison, WI, USA; [2]Laboratory for Optical and Computational Instrumentation, University of Wisconsin, Madison, WI, USA; [3]Cancer Sciences Unit, University of Southampton, Southampton, UK; [4]Department of Pathology, University of Wisconsin, Madison, WI, USA; [5]Paul P. Carbone Comprehensive Cancer Center, University of Wisconsin, Madison, WI, USA; [6]Department of Surgery, University of Wisconsin, Madison, WI, USA and [7]School of Pharmacy, University of Wisconsin, Madison, WI, USA

Pancreatic ductal adenocarcinoma continues to be one of the most difficult diseases to manage with one of the highest cancer mortality rates. This is due to several factors including nonspecific symptomatology and subsequent diagnosis at an advanced stage, aggressive metastatic behavior that is incompletely understood, and limited response to current therapeutic regimens. As in other cancers, there is great interest in studying the role of the tumor microenvironment in pancreatic ductal adenocarcinoma and whether components of this environment could serve as research and therapeutic targets. In particular, attention has turned toward the desmoplastic collagen-rich pancreatic ductal adenocarcinoma stroma for both biological and clinical insight. In this study, we used quantitative second harmonic generation microscopy to investigate stromal collagen organization and structure in human pancreatic ductal adenocarcinoma pathology tissues compared with non-neoplastic tissues. Collagen topology was characterized in whole-tissue microarray cores and at specific pathology-annotated epithelial–stroma interfaces representing 241 and 117 patients, respectively. We quantitatively demonstrate that a unique collagen topology exists in the periductal pancreatic ductal adenocarcinoma stroma. Specifically, collagen around malignant ducts shows increased alignment, length, and width compared with normal ducts and benign ducts in a chronic pancreatitis background. These findings indicate that second harmonic generation imaging can provide quantitative information about fibrosis that complements traditional histopathologic insights and can serve as a rich field for investigation into pathogenic and clinical implications of reorganized collagen as a pancreatic ductal adenocarcinoma disease marker.
Modern Pathology (2015) **28,** 1470–1480; doi:10.1038/modpathol.2015.97; published online 4 September 2015

Pancreatic ductal adenocarcinoma is one of the most devastating human malignancies. It is currently the fourth leading cause of cancer death and projects to become the second leading cause by 2030.[1] The 5-year relative survival rate has remained in the single digits for decades. Pancreatic ductal adenocarcinoma is notoriously difficult to detect before an advanced, inoperable stage is reached due to nonspecific symptomatology and the retroperitoneal location of the pancreas, which makes palpation or routine biopsy of suspicious masses difficult. Recent advances in the sensitivity and specificity of preoperative imaging modalities such as computer tomography, magnetic resonance imaging, positron emission tomography, endoscopic ultrasonography, and endoscopic retrograde cholangiopancreatography have played an important role in enhancing pancreatic ductal adenocarcinoma diagnosis, detailing the relationship of lesions to nearby anatomical structures, and determining the course of management.[2] Despite these advances, only 10–15% of patients are diagnosed at a localized disease stage when surgical resection is possible as a potential curative therapy. However, postsurgical recurrence rates are high with 5-year survival rate of

Correspondence: Dr WJ Kao, BS, MS, PhD, Department of Biomedical Engineering, Laboratory for Optical and Computational Instrumentation, Paul P. Carbone Comprehensive Cancer Center, University of Wisconsin, 7123 Rennebohm Hall, 777 Highland Ave, Madison, WI 53705, USA.
E-mail: wjkao@.wisc.edu
Received 27 March 2015; accepted 16 July 2015; published online 4 September 2015

only 10%, and the disease has a notable resistance to adjuvant therapeutic strategies.[3]

New insights into pancreatic ductal adenocarcinoma pathogenesis are critically needed to enhance clinical management and inform novel therapeutic targets. Pancreatic ductal adenocarcinoma tumors are characterized by an extensively desmoplastic stroma when examined histologically. This dense fibrosis can account for up to 90% of the overall tumor volume.[4] In a number of different cancer types, stromal properties have demonstrated importance in disease identification, progression, and patient prognosis.[5–12] Given the pronounced desmoplastic reaction in pancreatic ductal adenocarcinoma, a large number of recent research efforts have focused on elucidating stroma–cancer interactions for both nuanced insight into disease progression and for potential diagnostic, prognostic, or therapeutic targets.[13]

The dominant extracellular matrix component of most tumor stromas, including that of pancreatic ductal adenocarcinoma, is fibrillar collagen. Recent technological advances in nonlinear microscopy modalities such as second harmonic generation imaging[14] have enabled visualization of collagen-based changes at cellular resolution and provided unprecedented insight into tumor growth and metastasis.[15] Fibrillar collagens possess a unique non-centrosymmetric structure allowing them to act as a frequency doubler when interacting with multiphoton laser light. This coherent, nonabsorptive light interaction process can be exploited to obtain high-resolution, quantifiable images of discrete collagen fibers in a number of sources including two-dimensional histopathology specimens,[16] three-dimensional intact tissues,[17] and live animal models[18] without the need for exogenous staining. Using second harmonic generation imaging, a number of groups have shown that changes in collagen fiber structure and organization during tumor initiation and progression have biological consequences and correlate with clinical outcomes in a number of other solid tumor types.[19–21]

Although increased stromal collagen content has long been clinically documented in pancreatic ductal adenocarcinoma cases, its specific topology in relationship to the malignant glands has yet to be investigated in human tissue specimens. In this study, we utilized second harmonic generation imaging to interrogate and quantify collagen changes in relation to histologic features within pancreatic carcinomas. We demonstrate that a characteristic collagen topology exists in the stroma at the interface with malignant epithelium, and that specific collagen attributes provide quantitative parameters for distinguishing pancreatic ductal adenocarcinoma tissue from benign tissue, including both normal ducts and ducts in chronic pancreatitis. These findings validate a methodology and establish an important foundation to further decipher the biological and clinical implications of collagen topology as a pancreatic ductal adenocarcinoma disease marker.

Materials and methods

Human Tissue Microarrays

To assess collagen in different pancreatic tissue types, formalin-fixed paraffin-embedded human tissue microarrays were obtained commercially (US Biomax, Rockville, MD, USA). We also obtained additional human pancreatic tissue microarrays constructed from surgical specimens from patients that underwent resection for primary pancreatic ductal adenocarcinoma tumors at University Hospital Southampton. Human tissues were obtained between 2000 and 2010, under approval from the institutional review board (10/H0502/72). All tissues used in this study were derived from tumor excisions with curative intent (not diagnostic biopsies). Cases of hereditary pancreatitis or autoimmune pancreatitis were not included. Hematoxylin and eosin-stained slides were reviewed to confirm the diagnosis, and cases were excluded at this stage if it was unclear whether tumor originated from the pancreatic head or distal common bile duct. One to three cylindrical cores were taken from representative areas of each tumor block. Areas sampled included areas containing tumor islands, areas containing only tumor-associated stroma and surrounding areas with no evidence of tumor involvement as determined by a consultant pathologist.

Multiphoton Microscopy

Multiphoton laser-scanning microscopy was performed using a custom-built workstation at the University of Wisconsin Laboratory for Optical and Computational Instrumentation imaging research facility. All images were acquired using a Nikon Eclipse TE2000U inverted microscope through a Nikon S Fluor 20× air-immersion objective (numerical aperture = 0.75) (Nikon, Chiyoda, Tokyo). A mode-locked MIRA 900 Titanium:Sapphire laser (Coherent, Santa Clara, CA, USA) was tuned to an excitation wavelength of 890 nm to deliver ~10 mW of power at the sample. A Semrock 445 ± 20 nm narrow-band pass filter was used to isolate the backscattered second harmonic generation signal. Tissue microarrays were imaged in entirety using an acquisition grid defined in WiscScan, a laser-scanning software package developed at the Laboratory for Optical and Computational Instrumentation (http://loci.wisc.edu/software/wiscscan). Individual images of 512 × 512 pixels were acquired within the constraints of the grid with a 10% overlap between images. Following acquisition, a FIJI plugin[22] was used to stitch the images together based on OME-XML metadata.[23,24] Two-photon excited fluorescence images were also acquired without filtering in selected regions of interest.

Pathology Review

Hematoxylin and eosin-stained whole-tissue microarray cores were designated by pathology as either representing normal pancreas, chronic pancreatitis only (derived from pancreatic ductal adenocarcinoma cases but with no malignant elements present), or pancreatic ductal adenocarcinoma. Carcinoma tissues were assigned a histological grade according to the three-tier grading scheme by two pathologists. In total, tissues from 241 patients were considered. Select tissues (from 117 patients) were subjected to additional review by a pathologist (AL) to assess collagen changes in relation to relevant epithelial–stroma interfaces. Tissue microarrays were digitalized using an Aperio CS2 scanner system (Leica Biosystems, Buffalo Grove, IL, USA). Using ImageScope viewing software, normal ducts, ducts in chronic pancreatitis, and pancreatic ductal adenocarcinoma ducts were identified and annotated (1–3 annotations per core). Each annotation was the same size ($400 \times 400\ \mu m$), and representative regions were chosen where roughly a 1:1 epithelial–stroma proportion existed. The pathologists were blinded to the second harmonic generation data, thus eliminating the possibility that collagen visualization influenced how the tissues were reviewed and annotated.

Computational Collagen Fiber Segmentation and Quantification

Collagen fiber quantification was done using CT-FIRE, an open-source software package developed to automatically segment and quantify individual collagen fibers from second harmonic generation images (http://loci.wisc.edu/software/ctfire).[25] CT-FIRE was designed to compute the overall alignment of collagen fibers as well as individual length, straightness, and width. These fiber features were chosen because they appear to be altered in many cancer types compared with normal tissue counterparts.[19] Fiber length and width are calculated as pixel values. Alignment represents the overall directionality of fibers within the image on a scale from 0–1, where 1 indicates all fibers are orientated at the same angle. Straightness is calculated by dividing the distance between each fiber end point by the distance along the path of the fiber and is also on a scale from 0–1, where 1 indicates a perfectly straight fiber. For whole-core CT-FIRE analysis, individual stitched cores were first cropped using a 1.625 by 1.625 mm square region of interest tool in FIJI. For annotation CT-FIRE analysis, the regions drawn on the Aperio scans were transferred to the stitched cores and used to crop the second harmonic generation data prior to analysis. All images were eight-bit and thresholded 10–255 to eliminate background noise before running CT-FIRE using default parameters.

Alpha-Smooth Muscle Actin Immunohistochemistry

Automated immunostaining (Ventana XT, Ventana, Tucson, AZ, USA) was performed on representative pancreatic ductal adenocarcinoma tissue microarray cores from 39 patients for alpha-smooth muscle actin (1A4, Dako) in an accredited clinical cellular pathology department per the manufacturer's instructions as previously described.[26] The slide was digitalized using an Aperio CS2 scanner system and the Positive Pixel Count algorithm (v9) was used to quantify alpha-smooth muscle actin positivity in the individual cores.

Statistical Analysis

A linear mixed effects model with subject-specific random effects was developed in R statistical software (v3.1.1, www.r-project.org) and used to examine the association between tissue assignment and collagen fiber parameters. The results were summarized in terms of adjusted means and standard errors. Receiver operating characteristic curves were generated using MedCalc (v14.10.2, www.medcalc.org). All statistical tests were two-sided, and a confidence level of 95% was used to establish statistical significance.

Results

Quantification of Collagen Topology in Whole-Tissue Microarray Cores

The widespread clinical application of tissue microarrays has enhanced the efficiency with which diagnostic, prognostic, and therapeutic biomarkers are screened and assessed by accounting for tumor heterogeneity through increased patient representation.[27] Pathology-reviewed clinical tissue cores were imaged in entirety using a second harmonic generation stitching algorithm, which produced submicron resolution information about collagen distribution and topology in relation to epithelial structures. Even within standard diameter cores, a wide variety of histological features were qualitatively observed (Figure 1). For example, normal ducts were sparsely distributed among variable amounts of acinar and adipose tissue. In cores of chronic pancreatitis, the extent of fibrosis around the ducts varied considerably as well. Some ducts appeared similar to normal ducts, whereas some were contorted in the context of abundant collagen and superficially resembled malignant ducts.

Although pancreatic ductal adenocarcinoma tissues display an overall increase in fibrosis compared with benign tissues, we noted that the appearance of collagen was heterogeneous throughout individual cores. In some tumors, collagen appeared sparsely deposited around highly cellular regions, whereas in other specimens, highly aligned

collagen structures traversed the tissue with few intervening epithelial structures. In addition, the distribution of ductal epithelium (widespread *vs* sparse), different histological grades of the malignant glands, and occasional presence of blood vessels, nerves, adipose tissue, and infiltrating inflammatory cells contributed to the overall tissue heterogeneity of individual tissue cores.

The structure and organization of collagen fibers were objectively assessed in whole-tissue microarray cores by quantifying the corresponding second harmonic generation images. Despite the tissue heterogeneity observed in the tissue microarray cores, collagen fibers in the pancreatic ductal adenocarcinoma-associated stroma were significantly more aligned and longer than in normal pancreatic tissue, underscoring our initial qualitative observations (Figure 2). In addition, fibers in pancreatic ductal adenocarcinoma tissue were significantly more aligned than fibers in the setting of chronic pancreatitis ($P < 0.001$). When pancreatic ductal adenocarcinoma tissues were categorized by histological grade, a significant correlation between grade and collagen metrics was not observed (Supplementary Figure S1).

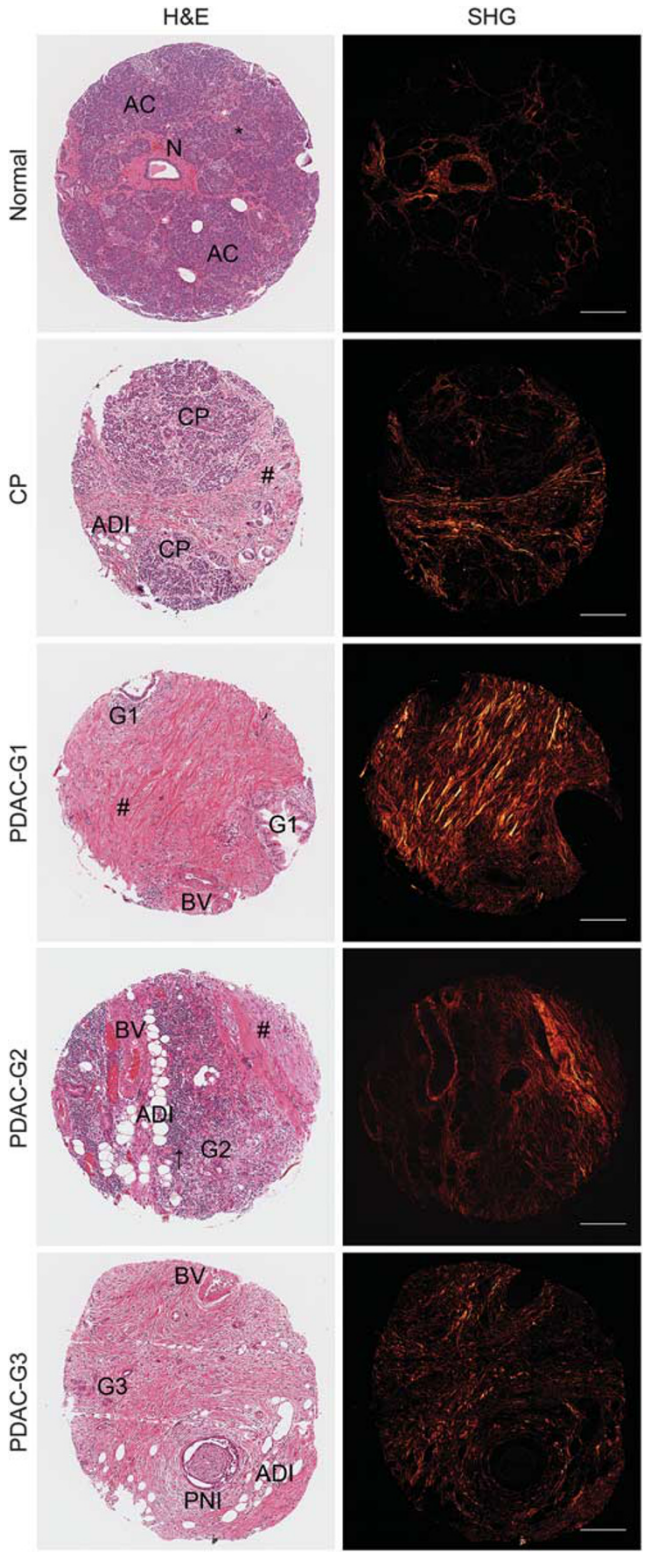

Figure 1 Pancreatic tissue heterogeneity. Whole-tissue microarray cores were visualized in entirety using traditional hematoxylin and eosin (H&E) histopathology (left column) and corresponding second harmonic generation (SHG) signal (right column, shown in red). Shown are representative cores determined to be as normal pancreatic tissue chronic pancreatitis, pancreatic ductal adenocarcinoma grade 1 (PDAC-G1), pancreatic ductal adenocarcinoma grade 2 (PDAC-G2), and pancreatic ductal adenocarcinoma grade 3 (PDAC-G3). Different tissue features and patterns of fibrosis are observed within single cores. AC, acinar tissue; ADI, adipose tissue; BV, blood vessel; CP, ducts in chronic pancreatitis; G1, well-differentiated (grade 1) pancreatic ductal adenocarcinoma duct; G2 = moderately differentiated (grade 2) pancreatic ductal adenocarcinoma duct; G3, poorly differentiated (grade 3) pancreatic ductal adenocarcinoma duct; N, normal duct; PNI, perineural invasion; ↑, inflammatory cell infiltration; *, connective tissue conforming to normal lobular architecture; #, highly aligned tracks of connective tissue. All images are shown at the same scale. Scale bar = 250 microns.

Stromal Collagen Topology Differs Around Distinct Pancreatic Tissue Features

Although tissue microarray cores have been shown to be representative samples of the entire tumor,[28] inherent tissue heterogeneity still exists. Without considering the spatial distribution of specific tissue components, it is unclear as to where characteristic collagen changes are occurring. To address this, we analyzed collagen in the immediate vicinity of structural elements within the tissue (ducts, blood vessels, nerves) and malignant epithelium, as identified by a pathologist on hematoxylin and eosin-stained material. Figure 3 depicts qualitative collagen attributes that were observed relative to different epithelial structures. Normal ducts are comprised of a single layer of cuboidal epithelium that contact an intact basement membrane that is maintained by resident pancreatic stellate cells.[29] Separating the normal duct from the rest of the

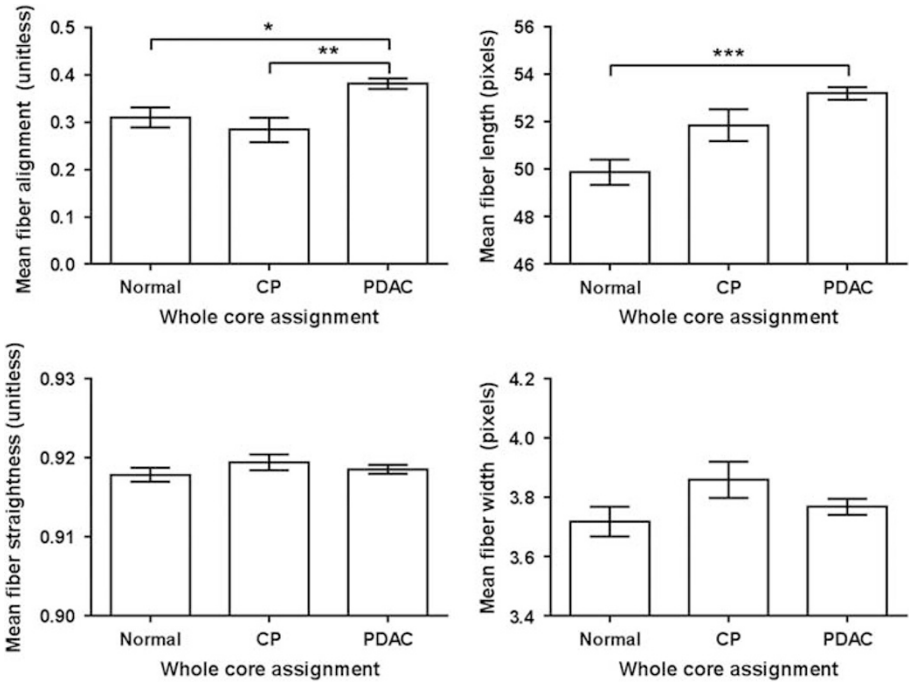

Figure 2 Quantification of collagen fiber alignment, length, straightness, and width in different pathology-reviewed whole-pancreatic tissue microarray cores. $n = 84$ normal, 49 chronic pancreatitis (CP), 508 pancreatic ductal adenocarcinoma (PDAC) cores from 241 patients. Data bars represent adjusted means ± standard error. $^{*}P < 0.05$, $^{**}P < 0.001$, $^{***}P < 0.0001$.

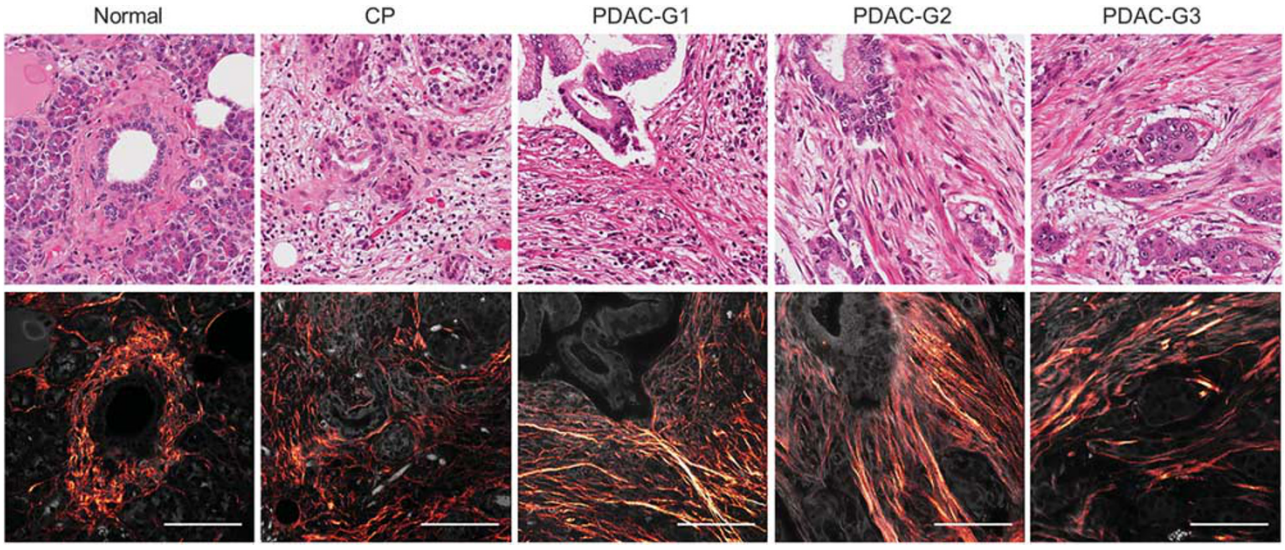

Figure 3 Key histological features of different representative stroma–epithelial interfaces in pancreatic tissue visualized using traditional hematoxylin and eosin (H&E) histopathology (top row) and corresponding second harmonic generation (SHG) signal (bottom row, shown in red). Normal ducts and benign ducts in chronic pancreatitis display a loose, concentric organization of collagen fibers around the epithelium. In pancreatic ductal adenocarcinoma tissues of all grades, cancer cells are surrounded by an ordered periductal stroma characterized by focally aligned and elongated collagen fibers. All images are shown at the same scale. Scale = 100 microns.

pancreatic parenchyma is a fibrotic cuff largely composed of short collagen fibers that are concentrically oriented around the duct lumen. Similar concentric collagen organization is observed in the stroma around blood vessels and nerves (Figure 4). In normal acinar tissue regions not in the immediate vicinity of ducts, collagen fibers are relatively sparse and when detected, conform to the normal lobular architecture of the pancreas. In chronic pancreatitis, ducts appear contorted and the periductal stroma is characterized by disorganized collagen fibers that interdigitate between the epithelial cells. Also, inflammatory cells are commonly observed dispersed throughout the immediately adjacent

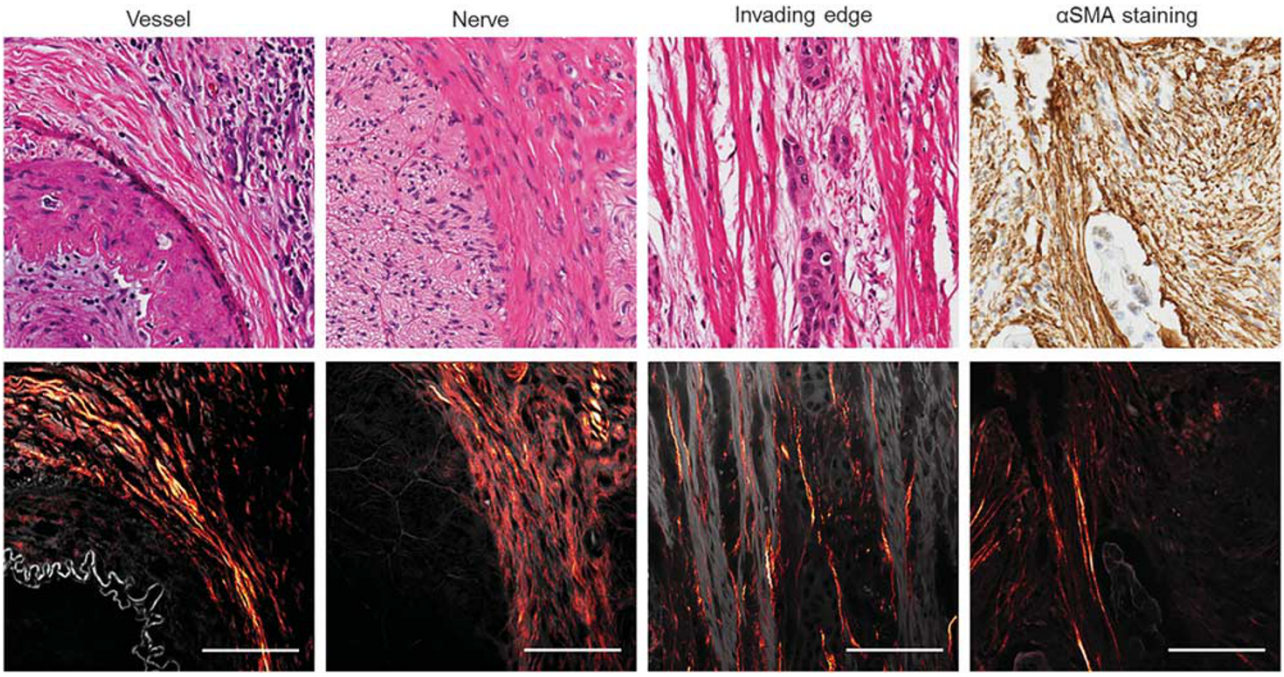

Figure 4 Key features of different tissue hallmarks in pancreatic tissue visualized using traditional histopathology (top row) and corresponding second harmonic generation (SHG) signal (bottom row, shown in red). First and second columns: normal blood vessels and nerves display a concentric organization of collagen fibers relative to the vessel lumen and nerve body, respectively. Third column: the front of a pancreatic ductal adenocarcinoma tumor infiltrating into the duodenal muscularis externa is characterized by distinct aligned and elongated collagen fibers orientated in the direction of invasion. Last column: immunohistochemical staining for alpha-smooth muscle actin (αSMA, brown) in pancreatic ductal adenocarcinoma tissue displaying the distribution cells relative to aligned and elongated collagen fibers running parallel to each side of a ductal protrusion. All images are shown at the same scale. Scale = 100 microns.

stroma. In areas of infiltrating pancreatic ductal adenocarcinoma, a significant increase in the overall density of fibers is readily apparent in all histological grades. The collagen of well-differentiated (grade 1) malignant ducts, which commonly resemble benign ducts if only epithelial atypia is considered, is strikingly more elongated and aligned in the immediate vicinity of the pancreatic ductal adenocarcinoma cells. Around moderately differentiated (grade 2) or poorly differentiated (grade 3) pancreatic ductal adenocarcinoma ducts, a similar collagen phenotype is observed. In our survey of 628 distinct pancreatic ductal adenocarcinoma regions, we saw that these collagen features can be either widespread or detected only at discrete foci around the epithelium. Interestingly, collagen also appeared reorganized at the infiltrating front of pancreatic ductal adenocarcinoma tumors, indicating a potential involvement of collagen reorganization in cancer cell invasion (Figure 4).

As collagen features appeared qualitatively distinct around ducts in three histologically distinct tissue types, we sought to determine whether quantitative parameters analyzed with CT-FIRE could distinguish whether a duct is normal, present in chronic pancreatitis, or malignant. Consistent with our whole-core analysis, the stroma of pancreatic ductal adenocarcinoma ducts showed statistically significant increases in collagen fiber alignment and length compared with normal and chronic pancreatitis stroma regardless of histological grade (Figure 5, Supplementary Figure S2). By focusing the analysis to the immediate vicinity of the epithelium rather than the entire stroma of the tissue core, we were able to achieve greater statistical power than with whole-core analysis. This underscores the inherent issue of tumor tissue heterogeneity and the need to account for the spatial distribution of cancer cells within the fibrotic stroma, and in relation to other, non-malignant cell types present. Furthermore, we saw that the pancreatic ductal adenocarcinoma stroma has collagen fibers that are significantly straighter and thicker, a finding that was not readily apparent in whole-core analysis. To determine which collagen fiber features are most powerful in discriminating duct types, we evaluated receiver operating characteristic curves. As shown in Figure 6 and Tables 1 and 2, a statistically significant difference was demonstrated between the pancreatic ductal adenocarcinoma and benign regions. Of the four collagen metrics, collagen fiber length had the most value in differentiating the regions with an area under the curve of 0.733 for pancreatic ductal adenocarcinoma *vs* benign and 0.701 for pancreatic ductal adenocarcinoma *vs* chronic pancreatitis. These findings indicate that a unique collagen topology can be detected in the pancreatic ductal adenocarcinoma stromal microenvironment on the basis of second harmonic generation imaging and

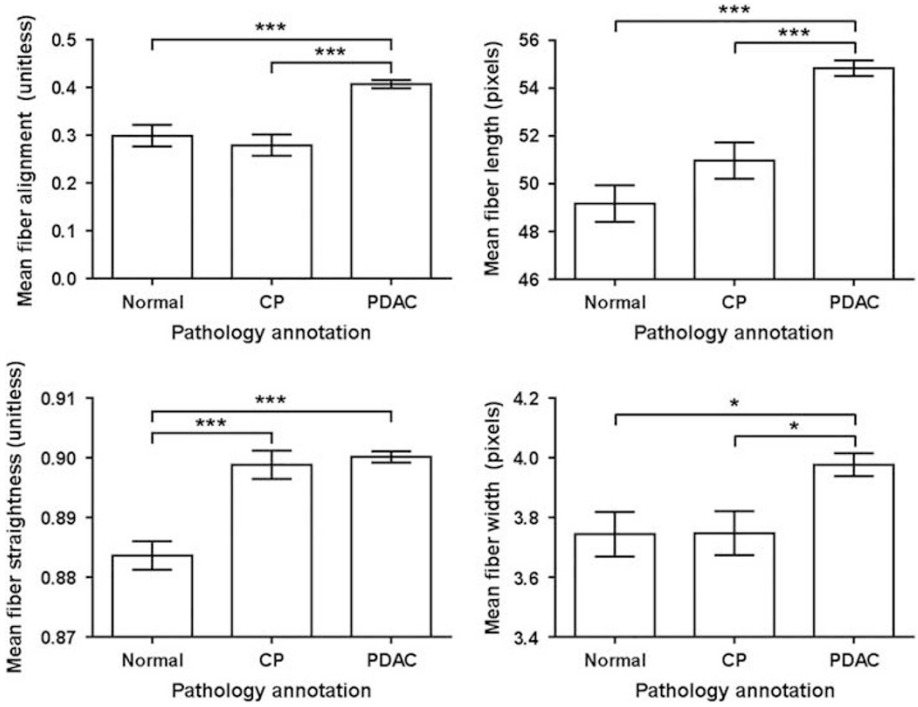

Figure 5 Quantification of collagen fiber alignment, length, straightness, and width in different pathologist-annotated periductal stroma types. $n = 67$ normal, 71 chronic pancreatitis (CP), 628 pancreatic ductal adenocarcinoma (PDAC) regions from 117 patients. Data bars represent adjusted means ± standard error. $^{*}P < 0.05$, $^{***}P < 0.0001$.

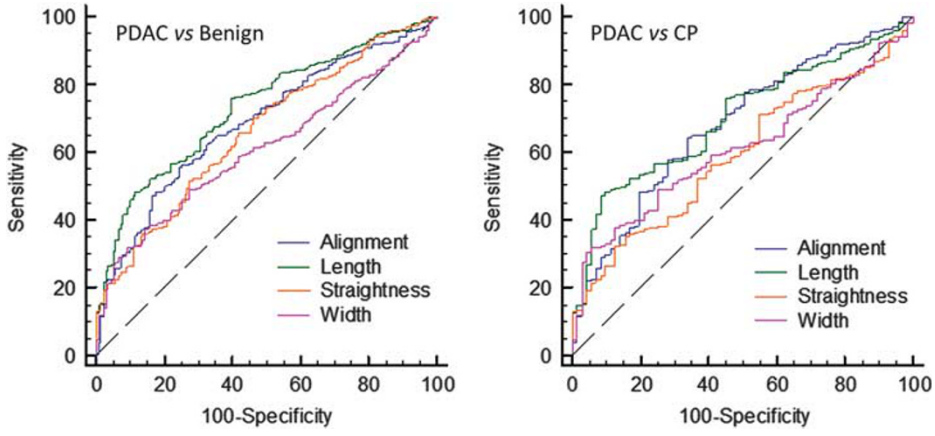

Figure 6 Receiver operating characteristic curves for differentiating stroma types based on collagen fiber features extracted by CT-FIRE. Left: pancreatic ductal adenocarcinoma (PDAC) regions *vs* benign regions (chronic pancreatitis and normal ducts). Right: pancreatic ductal adenocarcinoma regions *vs* only chronic pancreatitis (CP) regions. The line of no effect (area under the curve = 0.500) is shown as a dashed black line. $n = 67$ normal, 71 chronic pancreatitis, 628 pancreatic ductal adenocarcinoma regions from 117 patients.

Table 1 Receiver operating characteristic curve summary for collagen features distinguishing pancreatic ductal adenocarcinoma regions *vs* benign regions (chronic pancreatitis and normal ducts)

Collagen feature	*Area under the curve*	*95% confidence interval*	P-*value*	*Youden's index*	*Sensitivity*	*Specificity*
Alignment	0.686	0.652–0.719	< 0.0001	> 0.3864	55.6	75.4
Length	0.733	0.700–0.764	< 0.0001	> 54.7761	48.6	88.4
Straightness	0.661	0.626–0.694	< 0.0001	> 0.9006	52.2	71.2
Width	0.610	0.574–0.645	< 0.0001	> 4.1564	37.4	85.5

$n = 67$ normal, 71 chronic pancreatitis, 628 pancreatic ductal adenocarcinoma regions from 117 patients.

Table 2 Receiver operating characteristic curve summary for collagen features distinguishing pancreatic ductal adenocarcinoma regions *vs* only chronic pancreatitis regions

Collagen feature	*Area under the curve*	*95% confidence interval*	P-*value*	*Youden's index*	*Sensitivity*	*Specificity*
Alignment	0.681	0.645–0.716	<0.0001	>0.3344	64.2	66.2
Length	0.701	0.666–0.735	<0.0001	>54.9457	47.3	91.5
Straightness	0.593	0.555–0.630	0.0029	>0.9055	32.5	87.3
Width	0.611	0.574–0.648	0.0001	>4.2578	32.0	94.4

$n=71$ chronic pancreatitis, 628 pancreatic ductal adenocarcinoma regions from 117 patients.

quantification compared to normal pancreas and chronic pancreatitis.

Discussion

Histopathological evaluation of tumor tissue traditionally focuses on the epithelial elements when determining histologic type, grade, and stage for prognostic purposes.[30] The stroma is qualitatively appreciated but not conceptualized as an integral extension of the tumor, or considered as a quantitative disease marker. In this study, we systemically combined traditional pathology review and second harmonic generation imaging to interrogate stromal collagen structure and organization in normal and diseased pancreatic tissue. Our quantitative data demonstrate that a characteristic collagen topology exists in the pancreatic ductal adenocarcinoma stroma compared with that of normal ducts and ducts in the setting of chronic pancreatitis. At the histologic level, the profuse stroma production in chronic pancreatitis distorts the normal conformation of ducts, causing them at times to appear histologically similar to infiltrating pancreatic ductal adenocarcinoma. Our data showing a characteristic collagen topography in pancreatic ductal adenocarcinoma compared with chronic pancreatitis may be useful for the development of an ancillary histologic tool to help differentiate these two types of tissue changes. More importantly, the data suggest an important role for collagen organization during pathogenesis and progression of cancer.

To date, the specific pathophysiologic processes driving collagen reorganization in PDAC remain unclear. It has recently been shown that both the cellular and non-cellular composition of the periductal stroma changes dynamically during pancreatic ductal adenocarcinoma progression. Shi *et al* characterized the periductal stroma of ducts in chronic pancreatitis and pancreatic intraepithelial neoplasms, which are known to be precursor lesions to pancreatic ductal adenocarcinoma, through immunohistochemical staining of collagen, periostin, infiltrating macrophages, and activated alpha-smooth muscle actin-positive pancreatic stellate cells.[29] They demonstrated that low-grade pancreatic intraepithelial neoplasms show a marked increase in periductal collagen deposition without a large increase in periostin deposition or pancreatic stellate cell activation. As the pancreatic intraepithelial neoplasms evolve to higher grade lesions, the collagen density remains steady, but there is an increase in the number of activated pancreatic stellate cells. This stromal composition contrasts with that of chronic pancreatitis, where the stroma is known to be uniformly rich in periostin, collagen, macrophages, and pancreatic stellate cells. It is possible that increased activation of pancreatic stellate cells may result in the type of collagen remodeling in pancreatic ductal adenocarcinoma that our study demonstrates. In fact, many studies have shown that pancreatic stellate cells are crucial contributors to pancreatic ductal adenocarcinoma progression and are the principle source of fibrillar collagens, other extracellular matrix proteins, and soluble factors that promote the growth, invasion, metastasis, and survival of cancer cells.[31–36] In addition, the detection of pancreatic stellate cells immediately adjacent to pancreatic ductal adenocarcinoma epithelium correlates with adverse clinicopathological parameters.[6,7,37] Our group and others have shown that highly contractile pancreatic stellate cells can produce aligned collagen matrices *in vitro*, and the resultant topography can facilitate pancreatic ductal adenocarcinoma cancer cell migration.[38–40] Our immunohistochemical analysis suggests a positive correlation between alpha-smooth muscle actin expression and aligned collagen in the pancreatic ductal adenocarcinoma periductal stroma, which should be further validated on a larger patient cohort for potential mechanistic insight (Figure 4, Supplementary Figure S3). As second harmonic generation can be directly applied to histopathology specimens beyond those stained with hematoxylin and eosin, collagen topology analysis could be readily paired with other disease markers currently under investigation in pancreatic ductal adenocarcinoma for nuanced insight into pathogenesis.[41–43]

The pathological impact of changes in pancreatic ductal adenocarcinoma stroma collagen topology also remains unclear. Accumulating evidence suggests that focally aligned collagen at the stroma–cancer interface guides the persistent migration of cancer cells away from the tumor and toward vasculature during the metastatic cascade.[20,44–46] In addition, the detection of aligned collagen signatures in routine histopathology slides can predict disease

recurrence and patient survival in breast cancer patients.[16] In pancreatic ductal adenocarcinoma, cancer cells in contact with collagen type I show enhanced migratory capabilities through upregulation of Snail, a regulator of epithelial-to-mesenchymal transition.[47–51] Epithelial-to-mesenchymal transition is a process that dissemination-competent cells undergo. It has been shown to be prevalent in pancreatic ductal adenocarcinoma tissue and to negatively impact patient prognosis.[52] The potential functional link between collagen reorganization and increased pancreatic ductal adenocarcinoma cancer cell migration has yet to be elucidated.

Another potential pathological consequence of collagen reorganization in pancreatic ductal adenocarcinoma is increased matrix tension. Collagen is the preeminent scaffolding element in the human body, and alignment and cross-linking have been shown to increase tumor tissue stiffness levels.[53,54] Cells, in turn, are able to sense changes in the mechanical properties of the local environment and respond to them in ways that deviate from behaviors under normal tissue homeostasis.[55,56] Therapeutic targeting of lysyl oxidase in mouse models has shown promise in reducing collagen cross-linking and tumor stiffness, and ultimately in reversing the malignant phenotypes of cells.[57] Likewise, ablating mechanically interacting aligned collagen tracks between cancer cells results in a similar phenotype reversal.[58] Also related to increased tissue stiffness is the inability to systemically deliver therapeutics throughout pancreatic ductal adenocarcinoma tumors. Enzymatic and small molecule targeting of the periductal stroma has shown promise in remodeling the architecture, softening the tumor, decreasing interstitial pressure, and improving the efficiency of systemic delivery in pancreatic ductal adenocarcinoma.[59,60]

As last, disease markers that forecast which patients are most likely to experience accelerated progression or recurrence based on intrinsic tumor biology are critically needed to inform patient expectations, guide patient surveillance measures, and tailor personalized treatment regimens. There is emerging interest to stratify patients on the basis on stromal characteristics.[61,62] Stromal collagen topology has already been shown to correlate with breast tumors that have a greater propensity to metastasize and negatively impact prognosis.[16] It is likely that a diversity of collagen topology profiles exist in pancreatic ductal adenocarcinoma tumors, which may prove useful as an ancillary disease marker to subtype patients during histological evaluation. It is conceivable that collagen topology could be characterized from tissue obtained preoperatively (via endoscopic fine-needle aspiration or computer tomography-guided core needle biopsy) or post-resection using our validated methodology. This is currently an active area of study and is expected to add to our overall understanding of stroma–epithelial interactions during pancreatic ductal adenocarcinoma progression.

Acknowledgments

This study was supported by the University of Wisconsin School of Pharmacy with additional funding from the University of Wisconsin Laboratory for Optical and Computational Instrumentation. The authors thank the University of Wisconsin Translational Research Initiatives in Pathology Laboratory, in part supported by the University of Wisconsin Department of Pathology and Laboratory Medicine and the University of Wisconsin Carbone Cancer Center grant P30 CA014520, for use of its facilities and services. We also thank Dr Jens Eickhoff (Department of Biostatistics & Medical Informatics, University of Wisconsin–Madison) for providing guidance on statistical analysis.

Disclosure/conflict of interest

The authors declare no conflict of interest.

References

1 Rahib L, Smith BD, Aizenberg R *et al.* Projecting cancer incidence and deaths to 2030: The unexpected burden of thyroid, liver, and pancreas cancers in the United States. Cancer Res 2014;74:2913–2921.
2 Taylor B. Carcinoma of the head of the pancreas versus chronic pancreatitis: diagnostic dilemma with significant consequences. World J Surg 2003;27:1249–1257.
3 Hidalgo M. Pancreatic cancer. N Engl J Med 2010;362:1605–1617.
4 Neesse A, Michl P, Frese KK *et al.* Stromal biology and therapy in pancreatic cancer. Gut 2011;60:861–868.
5 Marsh D, Suchak K, Moutasim KA *et al.* Stromal features are predictive of disease mortality in oral cancer patients. J Pathol 2011;223:470–481.
6 Shi M, Yu DH, Chen Y *et al.* Expression of fibroblast activation protein in human pancreatic adenocarcinoma and its clinicopathological significance. World J Gastroenterol 2012;18:840–846.
7 Cohen SJ, Alpaugh RK, Palazzo I *et al.* Fibroblast activation protein and its relationship to clinical outcome in pancreatic adenocarcinoma. Pancreas 2008;37:154–158.
8 Conklin MW, Keely PJ. Why the stroma matters in breast cancer: insights into breast cancer patient outcomes through the examination of stromal biomarkers. Cell Adh Migr 2012;6:249–260.
9 Liu J, Liu J, Li J *et al.* Tumor-stroma ratio is an independent predictor for survival in early cervical carcinoma. Gynecol Oncol 2013;132:81–86.
10 Wang K, Ma W, Wang J *et al.* Tumor-stroma ratio is an independent predictor for survival in esophageal squamous cell carcinoma. J Thorac Oncol 2012;7:1457–1461.
11 Ayala G, Tuxhorn JA, Wheeler TM *et al.* Reactive stroma as a predictor of biochemical-free recurrence in prostate cancer. Clin Cancer Res 2003;9:4792–4801.
12 Underwood TJ, Hayden AL, Derouet M *et al.* Cancer-associated fibroblasts predict for poor outcome and promote periostin-dependent invasion in oesophageal adenocarcinoma. J Pathol 2014;235:466–477.

13 Erkan M, Hausmann S, Michalski *et al.* The role of stroma in pancreatic cancer: diagnostic and therapeutic implications. Nat Rev Gastroenterol Hepatol 2012;9: 454–467.
14 Campagnola PJ, Loew LM. Second-harmonic imaging microscopy for visualizing biomolecular arrays in cells, tissues and organisms. Nat Biotechnol 2003; 21:1356–1360.
15 Provenzano PP, Eliceiri KW, Keely PJ. Shining new light on 3D cell motility and the metastatic process. Trends Cell Biol 2009;19:638–648.
16 Conklin MW, Eickhoff JC, Riching KM *et al.* Aligned collagen is a prognostic signature for survival in human breast carcinoma. Am J Pathol 2011;178:1221–1232.
17 Hu WY, Zhao G, Wang CY *et al.* Nonlinear optical microscopy for histology of fresh normal and cancerous pancreatic tissues. PLoS One 2012;7:e37962.
18 Brown E, McKee T, diTomaso E *et al.* Dynamic imaging of collagen and its modulation in tumors *in vivo* using second-harmonic generation. Nat Med 2003;9: 796–800.
19 Keikhosravi A, Bredfeldt JS, Sagar AK *et al.* Second-harmonic generation imaging of cancer. Methods Cell Biol 2014;123:531–546.
20 Provenzano PP, Eliceiri KW, Campbell JM *et al.* Collagen reorganization at the tumor-stromal interface facilitates local invasion. BMC Med 2006;4:38.
21 Nadiarnykh O, LaComb RB, Brewer MA *et al.* Alterations of the extracellular matrix in ovarian cancer studied by Second Harmonic Generation imaging microscopy. BMC Cancer 2010;10:94.
22 Schindelin J, Arganda-Carreras I, Frise E *et al.* Fiji: an open-source platform for biological-image analysis. Nat Methods 2012;9:676–682.
23 Preibisch S, Saalfeld S, Tomancak P. Globally optimal stitching of tiled 3D microscopic image acquisitions. Bioinformatics 2009;25:1463–1465.
24 Linkert M, Rueden CT, Allan C *et al.* Metadata matters: access to image data in the real world. J Cell Biol 2010;189:777–782.
25 Bredfeldt JS, Liu Y, Pehlke CA *et al.* Computational segmentation of collagen fibers from second-harmonic generation images of breast cancer. J Biomed Opt 2014;19:16007.
26 Ward MJ, Thirdborough SM, Mellows T *et al.* Tumour-infiltrating lymphocytes predict for outcome in HPV-positive oropharyngeal cancer. Br J Cancer 2014;110: 489–500.
27 Kononen J, Bubendorf L, Kallioniemi A *et al.* Tissue microarrays for high-throughput molecular profiling of tumor specimens. Nat Med 1998;4:844–847.
28 Camp RL, Charette LA, Rimm DL. Validation of tissue microarray technology in breast carcinoma. Lab Invest 2000;80:1943–1949.
29 Shi C, Washington MK, Chaturvedi R *et al.* Fibrogenesis in pancreatic cancer is a dynamic process regulated by macrophage-stellate cell interaction. Lab Invest 2014;94:409–421.
30 Hartwig W, Hackert T, Hinz U *et al.* Pancreatic cancer surgery in the new millennium: better prediction of outcome. Ann Surg 2011;254:311–319.
31 Mantoni TS, Lunardi S, Al-Assar O *et al.* Pancreatic stellate cells radioprotect pancreatic cancer cells through β1-integrin signaling. Cancer Res 2011;71: 3453–3458.
32 Erkan MM, Reiser-Erkan C, Michalski CW *et al.* Cancer-stellate cell interactions perpetuate the hypoxia-fibrosis cycle in pancreatic ductal adenocarcinoma. Neoplasia 2009;11:497–508.
33 Hamada S, Masamune A, Takikawa T *et al.* Pancreatic stellate cells enhance stem cell-like phenotypes in pancreatic cancer cells. Biochem Biophys Res Commun 2012;421:349–354.
34 Xu ZH, Vonlaufen A, Phillips PA *et al.* Role of pancreatic stellate cells in pancreatic cancer metastasis. Am J Pathol 2010;177:2585–2596.
35 Erkan M, Adler G, Apte MV *et al.* StellaTUM: current consensus and discussion on pancreatic stellate cell research. Gut 2012;61:172–178.
36 Schneiderhan W, Diaz F, Fundel M *et al.* Pancreatic stellate cells are an important source of MMP-2 in human pancreatic cancer and accelerate tumor progression in a murine xenograft model and CAM assay. J Cell Sci 2007;120:512–519.
37 Fujita H, Ohuchida K, Mizumoto K *et al.* Alpha-smooth muscle actin expressing stroma promotes an aggressive tumor biology in pancreatic ductal adenocarcinoma. Pancreas 2010;39:1254–1262.
38 Lee HO, Mullins SR, Franco-Barraza J *et al.* FAP-overexpressing fibroblasts produce an extracellular matrix that enhances invasive velocity and directionality of pancreatic cancer cells. BMC Cancer 2011; 11:245.
39 Drifka CR, Eliceiri KW, Weber SM *et al.* A bioengineered heterotypic stroma-cancer microenvironment model to study pancreatic ductal adenocarcinoma. Lab Chip 2013;13:3965–3975.
40 Masamune A, Kikuta K, Satoh M *et al.* Rho kinase inhibitors block activation of pancreatic stellate cells. Br J Pharmacol 2003;140:1292–1302.
41 Ichihara T, Nomoto S, Takeda S *et al.* Clinical usefulness of the immunostaining of the tumor markers in pancreatic cancer. Hepatogastroenterology 2001;48: 939–943.
42 Ringel J, Löhr M. The MUC gene family: their role in diagnosis and early detection of pancreatic cancer. Mol Cancer 2003;2:9.
43 Shi C, Merchant N, Newsome G *et al.* Differentiation of pancreatic ductal adenocarcinoma from chronic pancreatitis by PAM4 immunohistochemistry. Arch Pathol Lab Med 2014;138:220–228.
44 Gritsenko PG, Ilina O, Friedl P. Interstitial guidance of cancer invasion. J Pathol 2012;226:185–199.
45 Condeelis J, Segall JE. Intravital imaging of cell movement in tumours. Nat Rev Cancer 2003;3:921–930.
46 Wang W, Wyckoff JB, Frohlich VC *et al.* Single cell behavior in metastatic primary mammary tumors correlated with gene expression patterns revealed by molecular profiling. Cancer Res 2002;62: 6278–6288.
47 Koenig A, Mueller C, Hasel C *et al.* Collagen type I induces disruption of E-cadherin-mediated cell-cell contacts and promotes proliferation of pancreatic carcinoma cells. Cancer Res 2006;66:4662–4671.
48 Armstrong T, Packham G, Murphy LB *et al.* Type I collagen promotes the malignant phenotype of pancreatic ductal adenocarcinoma. Clin Cancer Res 2004;10:7427–7437.
49 Ryschich E, Khamidjanov A, Kerkadze V *et al.* Promotion of tumor cell migration by extracellular matrix proteins in human pancreatic cancer. Pancreas 2009;38:804–810.
50 Shields MA, Dangi-Garimella S, Redig AJ *et al.* Biochemical role of the collagen-rich tumour

microenvironment in pancreatic cancer progression. Biochem J 2012;441:541–552.
51 Lu J, Zhou S, Siech M *et al.* Pancreatic stellate cells promote hapto-migration of cancer cells through collagen I-mediated signalling pathway. Br J Cancer 2014;110:409–420.
52 Yamada S, Fuchs BC, Fujii T *et al.* Epithelial-to-mesenchymal transition predicts prognosis of pancreatic cancer. Surgery 2013;154:946–954.
53 Levental KR, Yu H, Kass L *et al.* Matrix crosslinking forces tumor progression by enhancing integrin signaling. Cell 2009;139:891–906.
54 Plodinec M, Loparic M, Monnier CA *et al.* The nanomechanical signature of breast cancer. Nat Nanotechnol 2012;7:757–765.
55 Provenzano PP, Keely PJ. Mechanical signaling through the cytoskeleton regulates cell proliferation by coordinated focal adhesion and Rho GTPase signaling. J Cell Sci 2011;124:1195–1205.
56 DuFort CC, Paszek MJ, Weaver VM. Balancing forces: architectural control of mechanotransduction. Nat Rev Mol Cell Biol 2011;12:308–319.
57 Barry-Hamilton V, Spangler R, Marshall D *et al.* Allosteric inhibition of lysyl oxidase-like-2 impedes the development of a pathologic microenvironment. Nat Med 2010;16:1009–1017.
58 Shi Q, Ghosh RP, Engelke H *et al.* Rapid disorganization of mechanically interacting systems of mammary acini. Proc Natl Acad Sci USA 2014;111:658–663.
59 Provenzano PP, Cuevas C, Chang AE *et al.* Enzymatic targeting of the stroma ablates physical barriers to treatment of pancreatic ductal adenocarcinoma. Cancer Cell 2012;21:418–429.
60 Alvarez R, Musteanu M, Garcia-Garcia E *et al.* Stromal disrupting effects of nab-paclitaxel in pancreatic cancer. Br J Cancer 2013;109:926–933.
61 Erkan M, Michalski CW, Rieder S *et al.* The activated stroma index is a novel and independent prognostic marker in pancreatic ductal adenocarcinoma. Clin Gastroenterol Hepatol 2008;6:1155–1161.
62 Sinn M, Denkert C, Striefler JK *et al.* α-Smooth muscle actin expression and desmoplastic stromal reaction in pancreatic cancer: results from the CONKO-001 study. Br J Cancer 2014;111:1917–1923.

Supplementary Information accompanies the paper on Modern Pathology website (http://www.nature.com/modpathol)